اونيۏرسيتي مليسيا ڤهڠ
UNIVERSITI MALAYSIA PAHANG

ORIGINAL ARTICLE

An Experimental Investigation of Dimple-Texturing on the Tribological Performance of Hardened AISI H-13 Steel

G. Vignesh* and Debabrata Barik

Department of Mechanical Engineering, Karpagam Academy of Higher Education, Coimbatore, India, 641 021.

ABSTRACT – The fabrication of dimple-texture is essential for reducing friction and wear in frictional interaction pairs. The tribological characteristics of the frictional interaction pairs can be improved by controlling the dimple pattern, the depth to diameter ratio, and the area density ratio. In this study, the tribological characteristics of tungsten carbide discs with various dimple-texture patterns and hardened AISI H-13 steel pins are tested experimentally using a pin on disc wear tester to identify the wear mechanism. Laser marking technology was utilized to fabricate the dimple-textures such as circular arrays of the honeycomb pattern and spherical dimple-texture pattern with varying area density ratios. The impact of dimple-texture patterns is examined experimentally under dry testing conditions. Dimple-textured surfaces have a positive influence as compared to non-textured smooth surfaces. Particularly, the spherical dimple-textured pattern reduces frictional coefficient and wear rate by 45% and 51%, respectively, compared to non-textured smooth surfaces. The dimple-texture pattern and area density ratio control are essential features in dimple-texturing.

INTRODUCTION

In order to streamline the process of dimple-texture forming, numerous investigators have applied a wide range of procedures to fabricate the dimple-texture patterns and to investigate the tribological performance using a pin on disc wear tester, including manual indentation methods, laser marking techniques, elliptical vibration cutting, micro grinding, vibration-assisted dimple-texturing, electrical discharge machining, electrical chemical machining, and micro casting [1]. Laser marking techniques were widely employed to fabricate dimple-texture patterns due to their precise control and flexibility [2]. The dimple-texturing in frictional applications reduces wear and/or friction between the interactive elements [3]. The phenomenon of dimple-texturing introduces arrays of micro-cavities into tribo-contact surfaces, influencing the surface topography alterations. In [4], the influence of three dimple-texture patterns was experimentally studied using a ball-on-disk wear tester. They are concluded that tribological performance is closely proportional to the dimple-texture depth of 1 μm. In addition to dimple texturing, different kinds of surface topography alteration processes are available, including shot peening, garnet blasting, grinding, and polishing [5]. In [6], the elliptical vibration cutting process was used to fabricate the trapezoidal, sinusoidal, and zigzag dimple-texture patterns and grooves on hardened steel. Furthermore, the sinusoidal shape dimple-texture pattern significantly improves the tribological characteristics by reducing wear rate, COF, and tribo-pair adhesion.

Laser surface texturing (LST) modifies the surface properties of materials by infusing high thermal energy through a high-intensity laser beam to achieve the required tribological properties of metals, such as resistance to hardness and wear. As a result, the LST method is utilized as an alternative to the traditional heat treatment method to modify the surface of the metal to obtain the desired qualities without affecting the other properties of the materials [7]. In tribological applications, micro-cavities such as dimples, grooves, and scratches enhance the tribological performance, particularly in reducing wear and friction on the tribo-contact pairs. The micro-cavities are fabricated on the targeted sliding surface to serve as a lubricant reservoir and minimize the contact area between sliding contact pairs [8].

The tribological performance of dimple-textured surfaces can be improved by using solid lubricants during the interaction between tribo-contact pairs. For example, in [9], the influence of micro-dimples packed with solid lubricants on the frictional characteristics of a tribo-contact pair was investigated. They hypothesized that the graphite lubricants had a low frictional co-efficient because of the development of tribo-films on worn surfaces. Graphite and molybdenum-di-sulfate (MoS_2) are common solid lubricants used for high load and high-temperature applications. Additionally, MoS_2 exhibits various significant characteristics, including lubricity under high loads, fret safety, an anti-slip effect, wear resistance, and resistance to corrosion [10]. Laser dimple-texturing is frequently employed in tribological surface topography alterations with minimal deformation impacts. The modified microstructure surfaces exhibited greater wear resistance by minimizing abrasion wear on the tribo-contact pairs [11]. Micro-dimples produce a hydrophobic effect on the tribo-contact pairs; laser dimple-textures have several beneficial impacts on frictional interactions [12]. In [13], the groove textures were created by laser texturing on stainless steel, and the effect of pulse durations ranging from

nanoseconds to femtoseconds was investigated. They found that a laser pulse length of 400 femtoseconds significantly minimized thermal damage and heat-affected zone.

The microscopic study better understands propagation crack and wear mechanisms in different materials under various dimple-texture patterns [14]. The spiral arrays of dimple-texture patterns exhibit optimal results compared with circular arrays of dimple-texture patterns under identical loading conditions. When performing the tribology test in a dry condition, the micro-cavities are employed to capture the wear debris and minimize the area of contact to reduce wear and/or friction [15]. In [16], discovered that bi-triangular dimples with a 20% area density had a stronger impact on enhancing the tribological characteristics of contact pairs than other shapes and sizes. In [17], the influence of varying shapes of dimple-texture patterns on the surface morphology of frictional pairs was shown. According to the findings, the ellipsoidal texture with 300μm spacing has a minimal wear rate. In [18], recommended a micro-dimple size of 90 microns, a pitch of 135 microns, a depth of 10 microns, and a dimple area density of 35% based on the frictional test. In [19], compared the outcomes of non-textured samples with the laser dimple-textured samples and concluded that wear and friction were reduced up to a factor of 160 in comparison with non-textured samples. In [20], observed that a relatively small rise in wear rate was observed (from 15 N to 25 N), but a significant increase in wear rate was observed (from 25 N to 35 N) due to elevated temperature and pressure at the tribo-contact surfaces.

At low sliding velocities, dimple-texturing parameters had a discernible influence on wear and/or friction [21]. In dry circumstances, triangular micro-dimples with 7.5 percent area density strongly influence excellent tribological enhancements [22]. In [23], discovered that the elliptical-shaped dimple-texture patterns had the most significant wear and/or friction reduction effects, followed by the hemispherical and triangular dimple-texture patterns. Optimization methods were also used to determine the optimal geometries of dimple-texture patterns. The sloping bottoms of the textures provide efficient strategic converging wedge action, generating hydrodynamic pressure and enhancing the tribological performance [24]. In [25], it was recommended that the weighted signal-to-noise ratio can be used to obtain positive tribological outcomes using the multi-response optimization approach. In [26, 27], a dry sliding investigation on dimple-textured surfaces was performed to explore the wear process of dimple-textured surfaces. They discovered that a 5% increase in texture density resulted in a 27% decrease in wear rate. In [28], the dimple-texture patterns were analyzed, and inter-connecting line-like textures were observed. It is important to notice that the contacting surfaces are separated due to positive pressure fluctuation in the line-like textures. The information indicates that the textures' magnitude plays a critical role in reducing frictional coefficients by 35% compared to smooth surfaces [29].

Dimple-texturing is the process of forming micro-cavities on the contact surfaces of the frictional sliding pairs. Quantum research has been done on the different materials in diverse dimple-textures patterns such as dimple, convex, groove, pyramid, and petaloid [30]. Under the experimental conditions, a tribo-contact surface with an ellipse or triangular dimple-texture pattern has a lower load-carrying capability than a spherical dimple-texture pattern. Compared to untextured surfaces, higher frictional coefficients were recorded with pyramidal dimple-texture patterns [30]. The sloping bottoms of the spherical dimple-texture patterns provide efficient strategic converging wedge action, generating hydrodynamic pressure and enhancing the tribological performance [24]. The amount of heat-affected zone and tensile residual stresses around the dimple edge were increased with the convex and groove-shaped dimple-texture patterns. Frictional coefficient and wear rate were increased with the petaloid-shaped dimple-texture patterns due to high surface irregularities, which minimize the trapping of wear debris [33]. Honeycomb structures inspired by the snake-skin texture are appropriate for antifouling prevention, and this type of dimple-texture pattern is comparatively new. However, there is a research gap to identify the influence of dimple-texture patterns like honeycomb structures and spherical dimple texture on the tribo contact pairs. The laser marking method was used in this study to fabricate micro-dimples on tungsten carbide surfaces. The primary goal is to investigate the wear mechanism and friction behavior of laser dimple-textured surfaces with honeycomb dimple-texture patterns and spherical dimple-texture patterns under dry environments.

MATERIALS AND METHODS

Specimen Preparation

Figure 1 represents the CAD models of test specimens corresponding to honeycomb and spherical dimple-texture patterns with dimple area densities of 25% and 35%, respectively. The CAD models were designed in the 2D drafting module of AutoCAD and saved the drawing file in dfx format for further processing of files as inputs for the laser dimple-texturing. The total number of dimples (M) to be formed on the test specimen disk was estimated using the equation.

$$M = \frac{[(\pi S^2) \times q]}{[\pi s^2]} \tag{1}$$

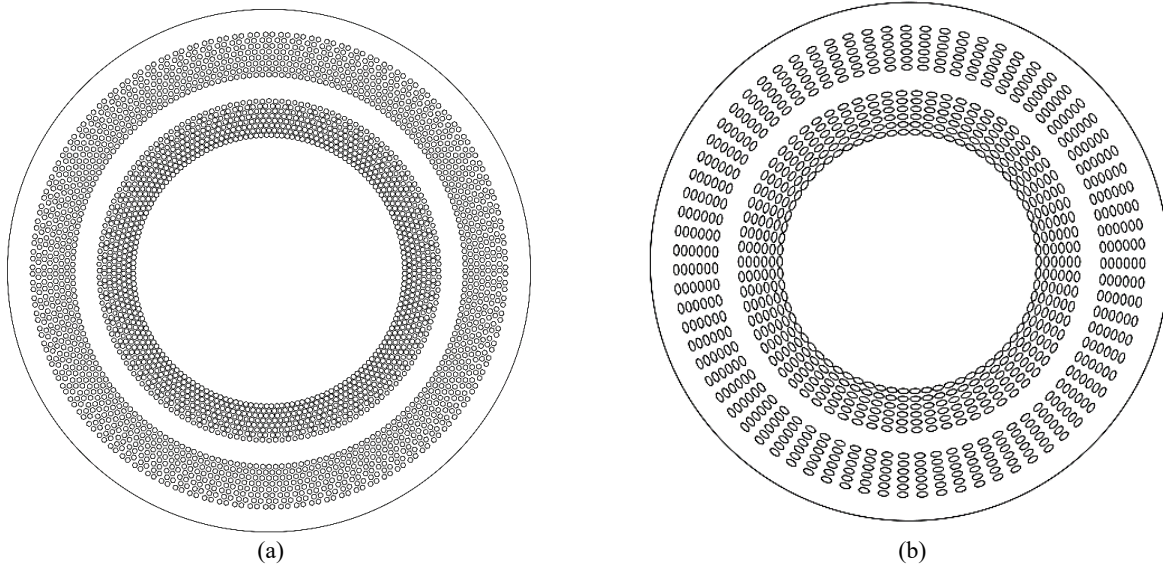where 'S' is the diameter of the test specimen disk, 'q' is dimple area density and 's' is the size of the dimple.

(a)   (b)

Figure 1. CAD drawings of dimple-textured disks of (a) honeycomb structure, (b) spherical dimple-texture type structure.
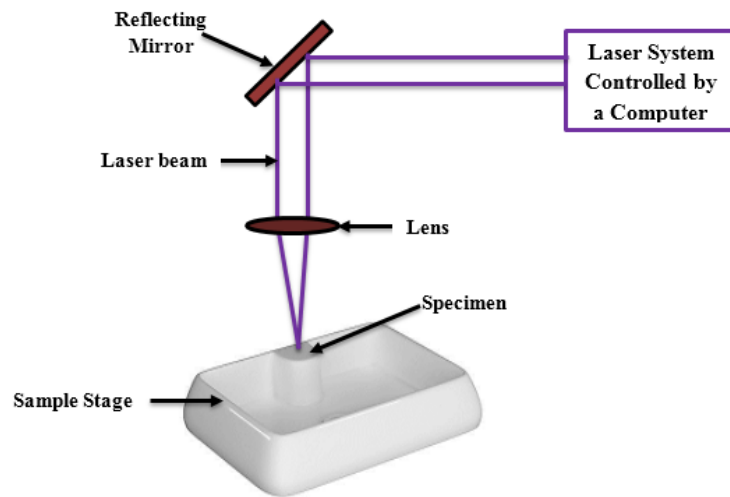

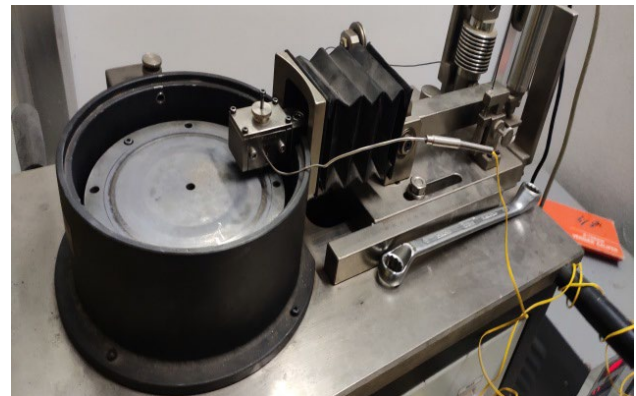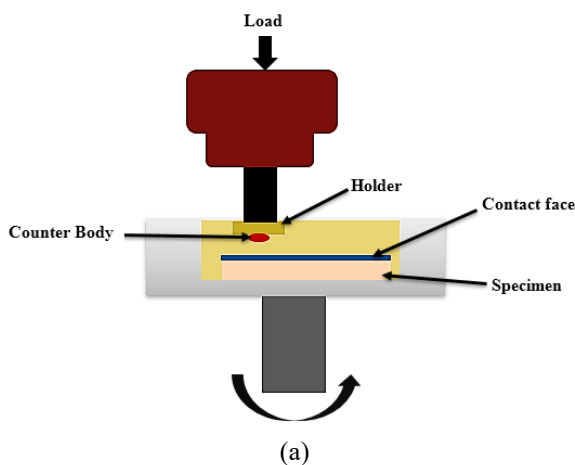**Figure 2.** Schematic representation of laser surface texturing.

(a)   (b)

Figure 3. (a) Schematic representation of the pin-on-disk rig, and (b) test rig apparatus.

A tungsten carbide disk of Ø180mm×10 mm and a cylindrical hardened AISI H-13 steel pin of Ø10 mm×25 mm was identified as the test specimens for wear test in a pin on disc wear tester. The chemical composition and mechanical properties of the tungsten carbide disk and AISI H-13 steel pin are listed in Table 1. and Table 2. respectively. Based on information obtained from the literature study, the diameter, depth, pitch, and area density ratio of the dimple-texture pattern were derived. The linear distance between two successive dimples is referred to as dimple pitch, and the ratio between the dimpled-textured area and the untextured area is defined as an area density ratio or dimple ratio [31]. Table

3. details the parameters of dimple-texture patterns. Subsequently, the tungsten carbide disk is polished with fine emery (grade 300) to eliminate protuberances at the dimple edges after laser marking and to ensure no residual debris within the micro-dimple cavity before conducting the wear test. The spiral array of the multi-dimple area density (q) is calculated using the equation.

$$q = \frac{\pi}{2\sqrt{3}} \left(\frac{s}{f}\right)^2 \times 100\% \tag{2}$$

Where 's' is the size of the dimple and 'f' is the dimple pitch size. Two dimple-texture patterns (Honeycomb and spherical dimple-texture) are employed for the wear test to investigate the effects of dimple-texture. The depth of the micro-dimple is maintained as 10 µm for all the textured patterns.
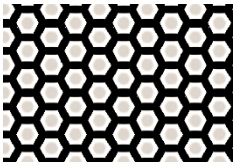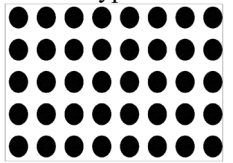
Table 1. Properties of tungsten carbide disk [31].

Element Name	Chemical composition (%)	Mechanical properties	Values
W	Balance	Tensile strength (MPa)	370 – 530
C	4.8 – 5.6	Yield strength (MPa)	600 – 686
Ni	8.5 – 11.5	Impact strength (J)	482 – 820
Cr	4.4 – 5.6	Hardness (BHN)	420 – 480
Fe	< 0.3	Elongation (%)	8

Table 2. Properties of AISI H-13 steel pin [32].

Element Name	Chemical composition (%)	Mechanical properties	Values
Cr	4.75 – 5.50	Tensile strength (MPa)	1200 – 1590
Mo	1.10 – 1.75	Yield strength (MPa)	1000 – 1380
V	0.80 – 1.20	Impact strength (J)	60 – 74
Si	0.80 – 1.20	Hardness (BHN)	290 – 370
C	0.32 – 0.45	Elongation (%)	11
Cu	0.25		
Ni	0.3		
Mn	0.20 – 0.50		
S	0.03		
P	0.03		

Table 3. Dimple-texturing parameters

Dimple properties	Texture Name		
Designation	Non-textured	Honeycomb	Spherical dimple-texture type
Structure of dimples	-		
Surface roughness (µm)	0.07 - 0.08	0.06 - 0.07	0.06 - 0.07
Pitch (µm)	-	135, 150	135, 150
Size of dimples (µm)	-	90	90
Dimple depth (µm)	-	10	10
Dimple area density (%)	-	25, 35	25, 35

The preferred dimple-texture patterns with optimal geometry are formed on a tungsten carbide disk using fiber laser marking machine 20W. Laser dimple texturing (LDT) is one of the most sophisticated dimple texturing methods for fabricating micro-cavities on the surfaces of the tribo-contact pairs. The dimple-texture patterns fabricated using laser are precise, extremely fast with minimal processing times [33]. It enables the development of optimum geometrical parameters by providing high precision control of size and form. It can be utilized for various materials, including metals, ceramics, and polymers. LDT has been employed in the electronics sector for more than two decades, particularly in magnetic disks and micro-electromechanical devices [34]. The texturing method uses a concentrated pulsed laser to create micro-dimple patterns surrounded by a solidified melt rim. Because of the enormous energy associated with LDT, material melting and vaporisation occur, resulting in heat-affected zone regions on the solidified melt rim, affecting the local microstructures and mechanical characteristics. The pulse repetition rate can be adjusted to reduce microstructural alterations and the size of the solidified melt rim. The recommended pulse repetition rate of 20 kHz is selected based on the literature study and experimentations to produce 10 µm dimple depth, as illustrated in Figure 2.

Moreover, in economic aspects, the cost of fabricating the dimple-textures using laser is low when compared to other precise methods like elliptical vibration cutting, micro grinding, vibration-assisted dimple-texturing, electrical discharge

machining, electrical chemical machining, and micro casting. In our region, Rs.500/hour is being charged for fabricating dimple-texture patterns using fiber laser marking machine 20W. The machining time purely depends on the dimple geometry and pattern.

Solid Lubricant Preparation and Friction Test

The wear test of non-textured and dimple-textured test specimens being performed under dry conditions using a pin on the disk wear tester. The tungsten carbide dimple-textured disk specimen has been rotated clockwise against the AISI H-13 steel pins under the predefined load conditions. Solid lubricants are critical in improving the tribological characteristics of frictional pairs. The test specimen disks are cleansed with acetone and cured at room temperature. The cloth rubbing method is employed to develop a thin layer of Molybdenum-di-sulfate (MoS_2) solid lubricant film on the tribo-contact surfaces of the non-textured and dimple-textured tungsten carbide test specimens. A small amount of particles is equally distributed over the cloth surface to perform the cloth rubbing method. Then a non-textured and dimple-textured tungsten carbide disk specimen is rubbed for 5 minutes with mild pressure. The thin layer of the solid lubricant film is controlled to be less than 1 μm. The same wear test is also performed in dry conditions without using a solid lubricant on the tribo-contact surface of both non-textured and dimple-textured tungsten carbide disk test specimens under identical test conditions.
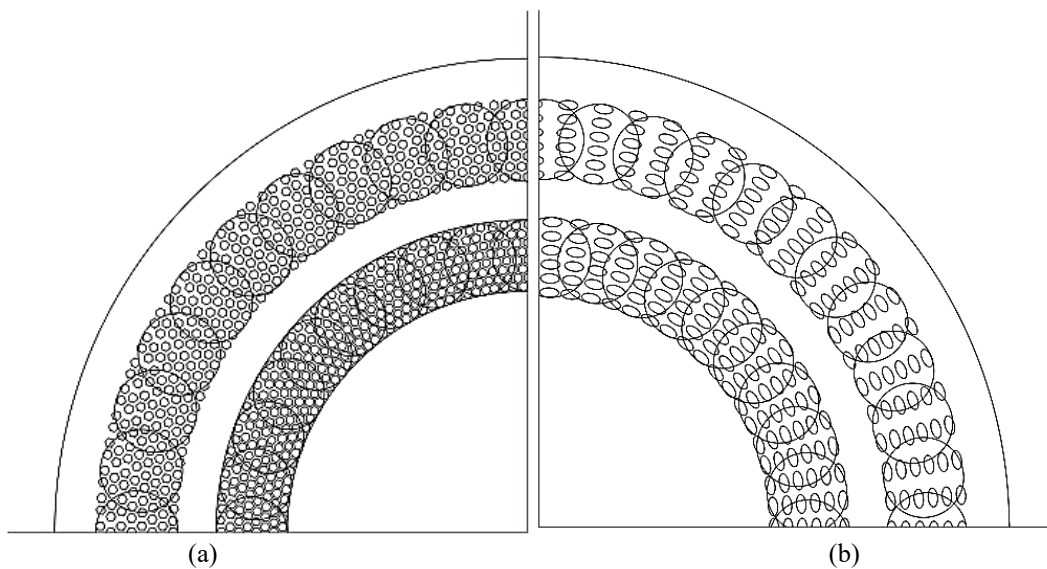

Figure 4. Tribo-pair contacts of (a) honeycomb structure, (b) spherical dimple-texture type structure.

Figure 3. illustrates the schematic representation of the pin-on-disk wear tester and test rig apparatus. This pin-on-disk wear tester is designed and developed specifically for rolling contact between a cylinder and planner interface, corresponding to the cam/follower method. Three different tungsten carbide disks are examined for wear and/or friction (smooth, honeycomb, and spherical dimple-texture). The cylindrical hardened AISI H-13 steel pin is inserted into the pin holder such that all DOF is controlled. The center of the cylindrical pin is properly loaded in the normal direction against the tungsten carbide disk placed under the steel pins. The disk is rotated at constant speed against the stationary steel pin. The wear test is carried out for three rotational speeds of 1000rpm, 1250rpm, and 1500rpm, while the normal load is maintained at 40N for all test runs. To prevent the initially imbalanced conditions, each wear test is performed for 10 minutes. A conception illustration of the tribo-contact area of micro-dimple surfaces with the hardened AISI H-13 steel pin for different dimple-texture patterns is depicted by a line diagram in Figure 4. The surface roughness of the polished test specimen disk and the pin is maintained within a range of Ra = 0.06 ~ 0.07μm. Before performing each wear test, the test specimens are cleaned with acetone and dried in ambient conditions. Each wear test is performed using a new surface of the tungsten carbide disk and ANSI H-13 steel pin under the atmospheric condition with an average temperature of 27 ± 2°C and relative humidity of 50-55%.

The frictional coefficient is recorded using software that interfaced with the pin-on-disk wear tester. The weight loss after a predetermined number of test cycles is determined by comparing the weight of test specimens before and after wear testing [35]. The weight loss is measured using an electronic weighing system with a 10-5 kg precision. Each wear test is conducted three times under the identical testing condition, with the mean results recorded. Worn-out tungsten carbide disk surfaces are examined using a 3D optical microscope to understand better wear mechanisms and the effect of dimple-texture patterns on wear and/or friction performance.

RESULTS AND DISCUSSION

Dimple-Textured Surface Morphology

Figure 5. shows the optical microscope images of the dimple-textured surfaces of the tungsten carbide disks with different dimple-texture patterns. Fiber laser marking machine 20W is utilized to fabricate the dimple-texture patterns on the tribo-contact surfaces of the tungsten carbide disk. The recommended pulse repetition rate of 20 kHz is selected based on the literature report [30] to minimize the heat-affected zone and tensile residual stresses around the dimple edge. The fabricated dimple-texture patterns are 10.0 ± 2.0 μm in-depth and 90.0 ± 2.0 μm in size. The relationship between the dimple depth and size ranges between $0.15 \sim 2$. These values are selected from the literature report [18] because it provides the minimum frictional force. After laser texturing, the cloth rubbing method is employed to develop a thin layer of Molybdenum-di-sulfate (MoS_2) solid lubricant film on the tribo-contact surfaces of the nontextured and dimple-textured tungsten carbide test specimens. The thin layer of the solid lubricant film is controlled to be less than 1 μm. Because of the variability of the burnished coatings and their thin thicknesses, lubricant films developed on the nontextured surfaces disappeared.

Furthermore, the film has limited adhesion due to the weak binding effect on the polished surfaces. As a result, the MoS_2 coating on the nontextured surfaces disappeared quickly. These findings are in line with the literature [10, 23]. Figure 5 clearly illustrates the development of a thin layer of MoS_2 film on the tribo-contact surface of dimple-textured and smooth nontextured test specimens. The micro-dimples have a significant percentage of solid lubricant traces, indicating that the micro-dimples operate as lubricant reservoirs. As the micro-dimples are retained with solid lubricants, the relative motion of the tribo-contact surfaces during the wear test causes significantly high pressure, resulting in the distribution of the solid lubricant to the adjacent surface. This generates a stable layer between the tribo-contact pairs, resulting in a reduced frictional coefficient. The pin on disk wear tester is used to evaluate the performance of spiral arrays of micro-dimples of honeycomb and spherical dimple-texture patterns with the pitch variation between uniformly formed micro-dimples and the variations in the dimple area density of 25% and 35%, in comparison with the smooth nontextured surfaces.
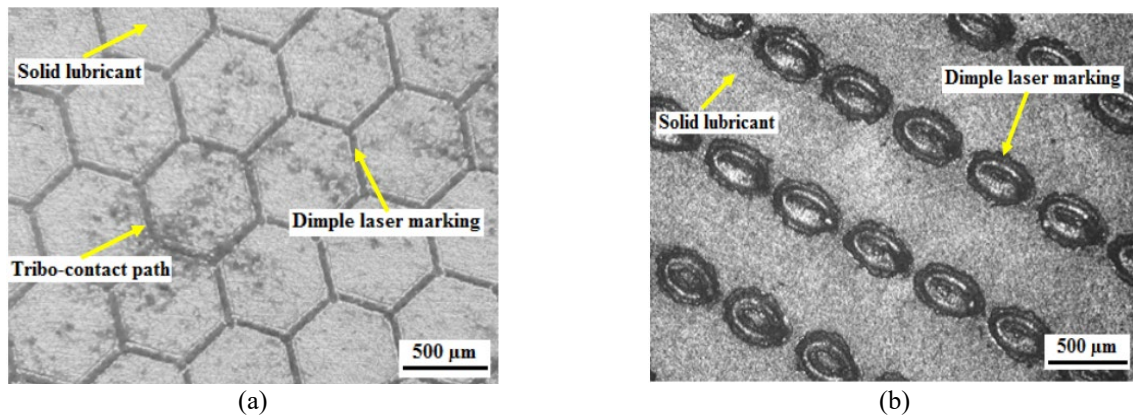

| (a) | (b) |

Figure 5. Optical microscope images of dimple-textured surfaces of (a) honeycomb structure, (b) spherical dimple-texture type structure.

The wear life of tribo-contact surfaces coated with solid lubricant is primarily influenced by the adherence of solid lubricant with the substrate and the retainability of the solid lubricant in the micro-cavities. Solid lubricant particles retain in the micro-cavities of dimple-texture surfaces under low contact pressure and uniform rubbing during the cloth rubbing method. The development of solid lubricant film in the space between the micro-dimples is facilitated by the mechanical interaction of solid lubricant particles in the rough surface and distributing the solid lubricant around the micro-dimples. Therefore, a minimal space between the micro-cavities should improve solid lubricant's spreading and retainability to the interface. In our experimental study, the reduced wear rate is recorded with a dimple-texture density of 35%. The investigation of the contact surfaces concludes that the failure of the solid lubricant film is identified by the retained quantity of solid lubricant in the region between the dimples, where the thickness of the solid lubricant film is relatively thin. The existence of the solid lubricant film between the tribo-contact pairs purely depends on the quantity of the solid lubricant retained in the micro-cavities. The significant benefit of solid lubricant film applied on dimple-textured surfaces over nontextured surfaces is that they have a higher load distribution of transition to seizure. Because of weak adherence, burnished coatings on the ground surface often have limited durability. Generally, solid lubricant coatings on nontextured surfaces have a short lifespan because of their weak adherence capability.

Effect of Dimple-Texturing on the Friction and Wear

Figure 6 shows the fluctuation of the frictional coefficient during the sample test duration (600 seconds) at a constant speed of 1500 rpm. The frictional coefficient readings for all test specimens are relatively equal to 200 seconds (steady-state period); after that, there is a dramatic increment in dry sliding without solid lubricant and a progressive increment in dry sliding with solid lubricant. The frictional coefficient value of the uncoated non-textured surface was unexpectedly raised from 0.2 to 0.75 within 100 seconds of test duration due to the severe abrasion wear developed on the tribo-contact

area of the frictional pairs. The measured friction and wear behavior for nontextured surfaces may be determined by the adhesion between the disk and the steel pin, accompanied by the development of wear debris due to relative motion. The wear debris is either trapped between the sliding surfaces or ejected from the contact due to centrifugal forces. In the case of nontextured surfaces coated with solid lubricant forms a thin layer between the tribo-contact surfaces during continued rubbing, it forms a competed layer on the interaction surfaces, resulting in a reduction in both frictions and wear by providing low-shear strength intersections at the interface and avoiding the interaction surfaces from direct metal to metal contact. These findings are in line with the literature [16]. In the case of dimple-textured surfaces, the micro-cavities can trap the wear debris grains, resulting in a lower wear rate than nontextured surfaces. The trapping of wear debris facilitates the smooth sliding at the tribo-contact interface because there is no loose wear debris available to cause abrasion wear and significantly reduce the frictional coefficient. When comparing uncoated tungsten disk and MoS_2 coated tungsten disk, the frictional coefficient in the MoS_2 coated tungsten disk is minimized due to the micro-dimple lubrication effect and the development of a thin layer of the solid lubricant on the tribo-pairs.
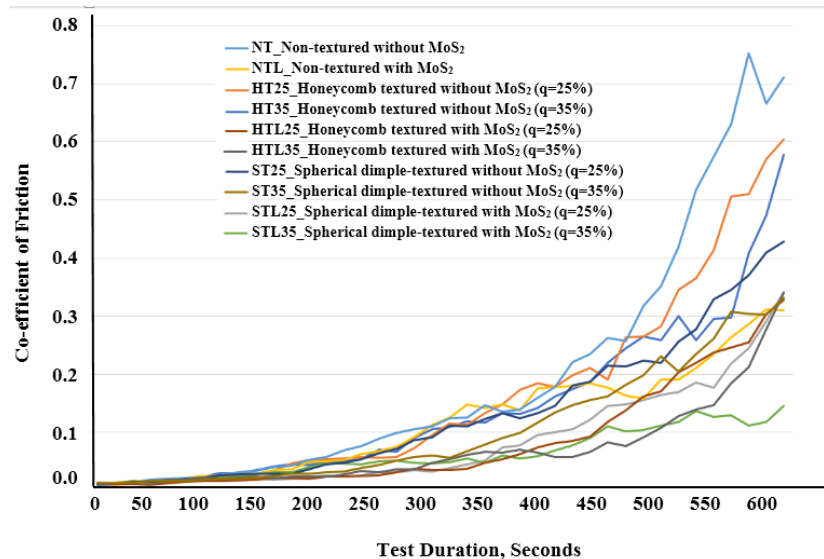

Figure 6. Variation of frictional coefficient with the test duration at a speed of 1500 rpm.

Effect of the Non-Textured and Dimple-Textured Surface on Tribological Properties under Dry Condition

Figure 7(a) illustrates the frictional coefficient of non-textured and dimple-textured surfaces at various rotating speeds under uncoated dry testing conditions. The friction test is carried out for 10 minutes with a constant load of 40N at rotational speeds of 1000 rpm, 1250 rpm, and 1500 rpm. The friction test demonstrates that when the area dimple density is significant, the frictional coefficient between dimple-textured and non-textured specimens is considerably different. The mean frictional coefficient is quite high at a low sliding speed of 1000 rpm for all dimple-textured disks but relatively low at a high sliding speed of 1500 rpm. This result explores the micro-cavities that had a more considerable influence on high-speed applications. The mean frictional coefficient at 1250 rpm is recorded to fall in-between. At the high rotational speed of 1500 rpm, the frictional coefficients are significantly reduced for HT35 and ST35 dimple-texture patterns. An identical variation trend could be identified for a rotational speed of 1250 rpm and 1000 rpm. Still, the frictional coefficients are comparatively low in all kinds of dimple-texture patterns when the rotational speed approaches 1500 rpm. The frictional coefficients are considerably high for NT and significantly low from HT25 to HT35 to ST25 to ST35, indicating that dimple area density and dimple-texture patterns significantly influence the friction reduction.

The pin on the disk wear tester is used to measure the wear rate for each test run, and the measurements are recorded in real-time. Figure 7(b) shows the wear rate measurements for non-textured (NT) and dimple-textured test specimens (HT25, HT35, ST25, and ST35) having various texture patterns and dimple area density at different rotational speeds of 1000, 1250, and 1500 rpm. The wear test outcomes reveal that dimple-textured samples had the lowest wear rate compared to non-textured samples at all rotational speeds. At rotating speeds of 1000 and 1250 rpm, the wear rate drops slightly or remains constant when the dimple area density increases from HT25 to HT35. Dimple-texture patterns like HT35 and ST35 exhibit excellent performance in minimizing wear rate because the maximum effective area of micro-cavities is employed to entrap the wear debris and reduce wear rate. Simultaneously, non-textured samples exhibit a higher wear rate because no feature is employed to entrap the wear debris. Because of bulges of micro-dimples at lower rotational speeds, the wear rate is significantly high; however, the bulges dissipate, and the development of a thin oxide layer on the tribo-contact surfaces at higher rotational speeds leads to minimizing the wear rate.
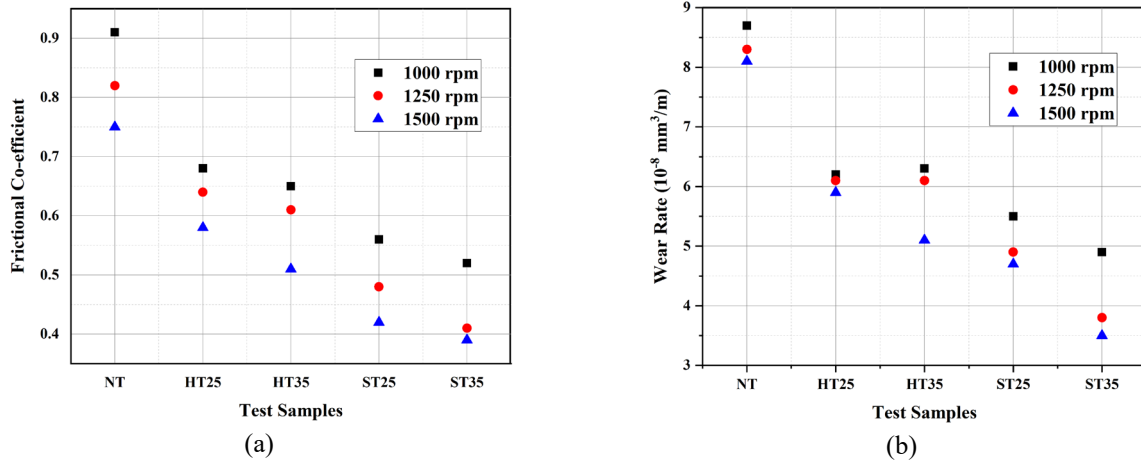
Figure 7. (a) Coefficient of friction and (b) wear rate under dry condition.

Effect of the Non-Textured and Dimple-Textured Surface on Tribological Properties under Solid Lubricant Condition

Figure 8(a) illustrates the variation in frictional coefficients of non-textured and dimple-textured patterns with varying rotational speeds under the coated solid lubrication (MoS$_2$) film. The results indicate that dimple-textured surfaces positively impacted frictional coefficient reduction. The study-state period stimulates MoS$_2$ film development on the contact surfaces of the tribo-contact pairs. The MoS$_2$ deposited in the micro-dimples can increase the wear resistance of the tribo-contact pairs. Even though the influence tribological performance of non-textured and dimple-textured surfaces with different dimple area densities shows the non-linear behavior, the frictional coefficient values exhibit a linear relationship with the variation in rotational speed. It clearly shows that the frictional coefficient value is reduced with an increase in rotational speed. When the rotating speed is minimal, the mean value of the frictional coefficient is relatively high, and the frictional force tends to decrease as the rotational speed increases. The frictional behavior of non-textured surfaces exhibited high variations in rotating speed variations. The frictional coefficient is measured for a 40N applied load on non-textured and dimple-textured surfaces. The mean frictional coefficient values of dimple-texture patterns like HTL35 and STL35 under the MoS$_2$ coated condition exhibit a minimal and stable frictional coefficient of 0.22 ~ 0.25 and 0.15 ~ 0.20, respectively, while a maximum frictional coefficient of 0.41 ~ 0.45 is observed for non-textured smooth surfaces. The mean frictional coefficient of the ST textured test specimens is significantly lower than the mean frictional coefficient of the HT textured test specimens at the identical rotational speed. Compared to non-textured surfaces, the mean friction coefficient of HT and ST textured surfaces is decreased by 30 ~ 35% and 40 ~ 4%, respectively. The findings clearly show that the size of the textures has a significant influence in reducing frictional coefficients by around 35% compared to non-textured surfaces.
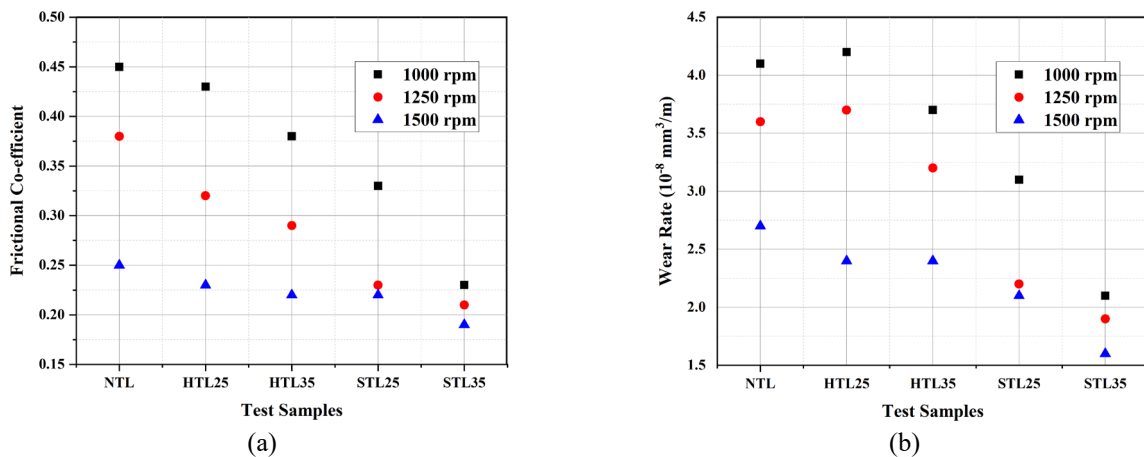

Figure 8. (a) Coefficient of friction and (b) wear rate under solid lubrication.

From the experimental test runs, the influence of area dimple density on wear rate at different rotational speeds is illustrated in Figure 8(b). The experimental outcomes indicate that dimple-texture patterns like HTL and STL have a lower wear rate when compared to NTL. The wear behavior exhibited higher fluctuations in non-textured smooth surfaces in all rotating speeds. The wear rate is recorded for a 40N applied load on non-textured and dimple-textured surfaces with MoS$_2$ coating conditions. Under rotational speed of 1500 rpm, the solid lubricant-coated dimple-textured surfaces resulted in a minimal, steady wear rate of nearly 1.6, 2.1, 2.4, and 2.4×10^{-8} mm^3/m for STL35, STL25, HTL35, and HTL25, respectively. It clearly states that MoS$_2$ coated dimple-texture patterns significantly improve the tribological performance

of the tribo-contact pairs. The micro-cavities in the dimple-texture patterns retain the solid lubricant, which minimizes heat generation at the frictional contacts. It might be the most important factor in minimizing adhesive wear for MoS_2-coated dimple-textured surfaces compared to uncoated dimple-textured surfaces and non-textured surfaces. Furthermore, the high dimple area density of the spherical dimple-texture type micro-dimples facilitates the formation of a solid lubricant thin layer on the tribo-contact surfaces. As a result, a spherical dimple-texture-type textured pattern has a considerable reduction in frictional coefficient and wear rate of roughly 45% and 51%, respectively, compared to non-textured smooth surfaces.

During the comparative examination on both instances (under dry and solid lubricant conditions), the performance of the micro-dimples exhibited a linear connection with the variation in rotational speed. Furthermore, in both circumstances, the higher dimple area density (35%) outperforms, the lower dimple area density (25%) because the effective area of contact between the tribo-contact pair is minimal in the higher dimple area density dimple-textures patterns. From the experimental runs, the low to high frictional coefficient and wear rate measured under dry condition is 0.37 – 0.92 and $3.56 – 8.72 \times 10^{-8}$ mm^3/m, the low to high values of frictional coefficient and wear rate measured under solid lubricant condition is 0.18 – 0.49 and $1.60 – 4.21 \times 10^{-8}$ mm^3/m. It reveals that MoS_2 coated surfaces perform significantly better than uncoated surfaces, with a 46 ~ 51% improvement in reducing frictional coefficient and a 51 ~ 55% improvement in reducing wear rate due to the micro-dimple lubrication effect and the formation of a thin layer of solid lubricant on the tribo-contact pairs.

Wear Mechanism

Figure 9 illustrates optical microscope images of non-textured and dimple-textured surfaces under dry and solid lubricant conditions. The surface topography of the uncoated non-textured specimen in Figure 9(a) changes significantly after the wear test due to the excessive occurrence of adhesive and abrasive wear. Compared to the MoS_2 coated non-textured surface, the intensity of wear rate in the MoS_2 coated dimple-textured surfaces is significantly reduced (Figure 9(b)). The contact surface of the MoS_2 coated honeycomb texture (Figure 9 (d)) experiences practically no damage due to creating a solid lubricant layer. Still, the uncoated honeycomb texture (Figure 9 (c)) experiences wear damage after the friction test, and laser marking is almost extinct. In the case of spherical dimple-texture (Figure 9(e) and 9(f)), the micro-dimples are evident in both coated and uncoated conditions because wear debris is retained in the micro-cavity, preventing additional wear. The micro-cavities are not completely visible, but it has a very low wear rate and minor distortions in surface topography after the wear test. Compared to the honeycomb structure, there is sufficient space to retain the solid lubricant; it is obvious that the spherical dimple-texture can retain the solid lubricant for a longer duration according to wear reduction.
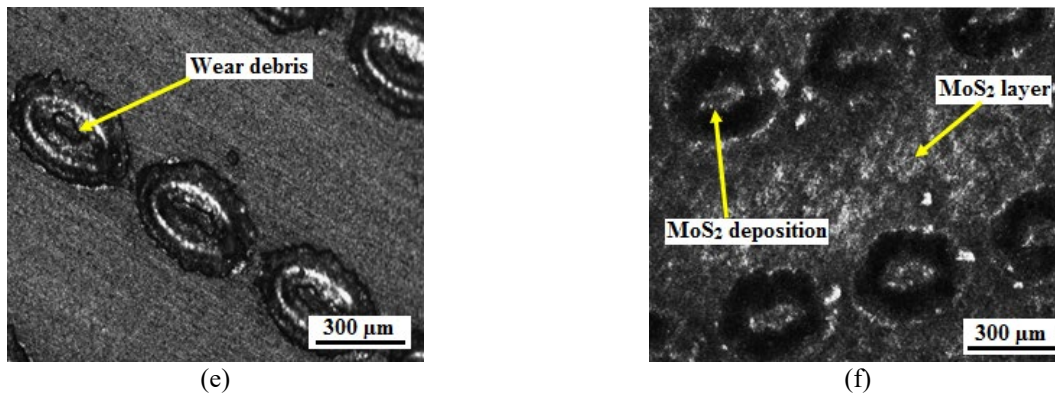

(a)

(b)

(c)

(d)

<center>(e)</center>

<center>(f)</center>
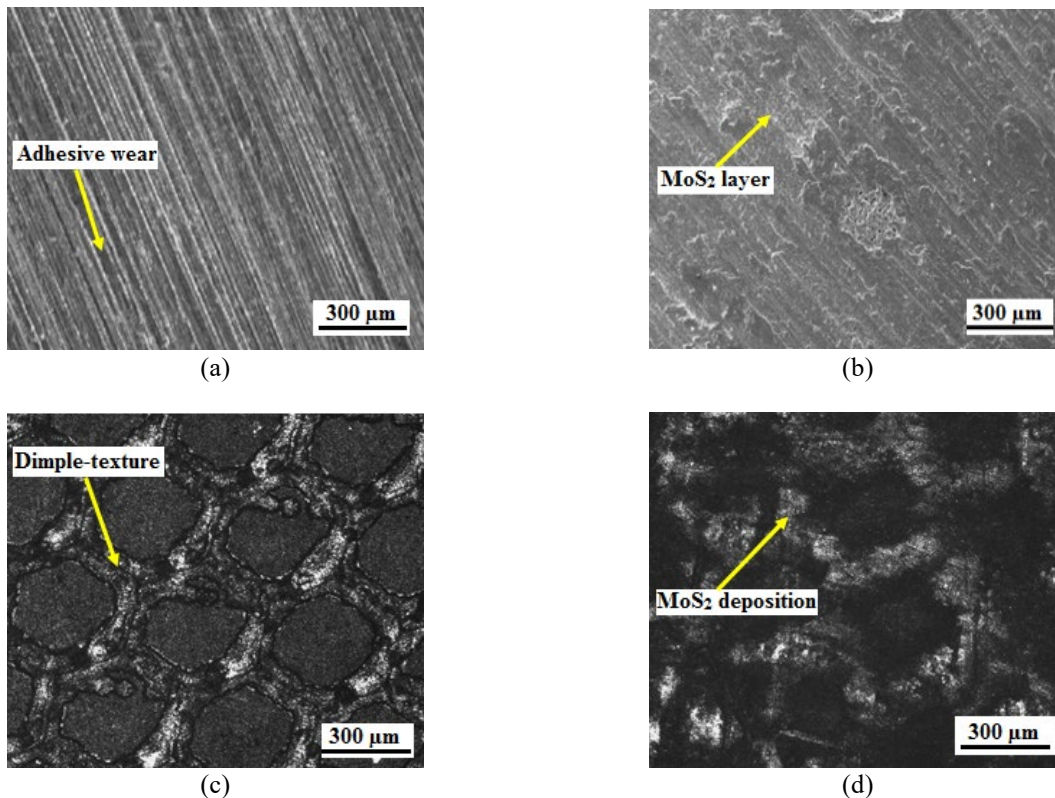
Figure 9. Optical microscope images of specimens after friction test (a) NT, (b) NTL, (c) HT, (d) HTL, (e) ST, (f) STL.

The spherical dimple-texture pattern has a micro-wedge bottom, which influences the formation of thick MoS_2 film than the flat bottom in the honeycomb dimple-texture pattern. Furthermore, the low to high values of wear rate recorded in a honeycomb dimple-texture pattern and spherical dimple-texture pattern under dry condition is $6.10\text{-}6.32\times10^{-8}$ mm³/m and $2.40\text{-}4.81\times10^{-8}$ mm³/m, respectively. The low to high values of wear rate recorded in a honeycomb dimple-texture pattern and spherical dimple-texture pattern under solid lubricant condition is $3.31\text{-}3.72\times10^{-8}$ mm³/m and $1.60\text{-}2.21\times10^{-8}$ mm³/m respectively. It indicates that MoS_2 coated spherical dimple-texture patterns perform much better than honeycomb dimple-texture patterns, resulting in a 40~45% wear reduction in dry condition and a 43~49% wear reduction in dry solid lubricant condition. As a result, spherical dimple-texture surfaces can be more efficient than honeycomb and non-textured tungsten carbide disc surfaces. More scratches and layer delamination are directly visible in non-textured surfaces after the wear test, indicating evidence of mixed wear (adhesive and abrasive wear). Because of the micro-cavities employed to capture wear debris and reduce contact area, the MoS_2 coated micro-dimple texture surface has a lower wear rate and practically zero-layer delamination.

DISCUSSION

The experimental findings indicated that all dimple-textured specimens with varying area density ratios successfully minimized the frictional coefficient. For nontextured smooth surfaces, a huge amount of adhesions and scuffing are observed on the tribo-contact surfaces after the wear test. However, for the dimple-textured test samples, the wear rate is significantly minimal compared with nontextured samples. In addition, there is no significant scuffing or adhesions developed on the tribo-contact surfaces after the wear test. The findings suggested that the influence of the trapping of wear debris facilitates the smooth sliding at the tribo-contact interface because there is no loose wear debris available to cause abrasion wear and significantly reduce the frictional coefficient. These findings are in line with the literature [29]. Dimple-texture patterns like HT35 and ST35 exhibit excellent performance in minimizing wear rate because the maximum effective area of micro-cavities is employed to entrap the wear debris and reduce wear rate. Simultaneously, nontextured samples exhibit a higher wear rate because no feature is employed to entrap the wear debris. Because of bulges of micro-dimples at lower rotational speeds, the wear rate is significantly high; however, the bulges dissipate, and the development of a thin oxide layer on the tribo-contact surfaces at higher rotational speeds leads to minimizing the wear rate.

Additionally, MoS_2 coated dimple-texture patterns significantly improve the tribological performance of the tribo-contact pairs. The micro-cavities in the dimple-texture patterns retain the solid lubricant, which minimizes heat generation at the frictional contacts. The solid lubricant retained in the micro-cavities is utilized to generate a second lubrication source to improve the tribological performance of the tribo-contact pairs in mixed or boundary lubrication. It might be the most important factor in minimizing adhesive wear for MoS_2-coated dimple-textured surfaces compared to uncoated dimple-textured surfaces and non-textured surfaces. The tribological performance on dimple-textured specimens is influenced by the area density ratio related to the lubrication compensation of adjacent dimples. Furthermore, the high dimple area density of the spherical dimple-texture type micro-dimples facilitates the formation of a solid lubricant thin layer on the tribo-contact surfaces.

In the literature on analyzing the effect of tribological performance of dimple-textured surfaces in common, the mechanisms most often stated are trapping wear debris [3, 15], micro hydrodynamic lubrication effect [26], and additional lubrication source [10, 29]. In dimple-textured surfaces, the micro-cavities can trap the wear debris grains, resulting in a lower wear rate than nontextured surfaces. The sloping bottoms of the dimple-textures provide efficient strategic converging wedge action, generating hydrodynamic lubrication effect and enhancing the tribological performance. The sloping bottoms of the spherical dimple-texture patterns provide efficient strategic converging wedge action, generating hydrodynamic pressure and enhancing the tribological performance. Likewise, solid lubricants retained in the micro-cavities are utilized to generate an additional lubrication source to improve tribological performance. As the micro-dimples are retained with solid lubricants, the relative motion of the tribo-contact surfaces during the wear test causes significantly high pressure, resulting in the distribution of the solid lubricant to the adjacent surface. Therefore, a minimal space between the micro-cavities should improve solid lubricant's spreading and ratainability to the interface. In our experimental study, the reduced wear rate is recorded with a dimple-texture density of 35%.

As a result, spherical dimple-texture surfaces can be more efficient than honeycomb and non-textured tungsten carbide disc surfaces. More scratches and layer delamination are directly visible in non-textured surfaces after the wear test, indicating mixed wear (adhesive and abrasive wear). Because of the micro-cavities employed to capture wear debris and reduce contact area, the MoS_2 coated micro-dimple texture surface has a lower wear rate and practically zero-layer delamination. Furthermore, laser dimple marking can act as heat treatment for test specimens, resulting in improved micro-hardness. The micro-cavities are employed to accumulate worn debris. Finally, the dimple-texture patterns exhibit consistent stress concentration throughout the tribo-contact surfaces, resulting in excellent wear resistance.

Comparing the tribological performance of spherical and honeycomb dimple-texture patterns reflects that the spherical dimple-texture patterns are more efficient in minimizing both the wear and friction and that too with a high area density ratio of dimples as obvious from Figures. 7, 8, 9, and 10. However, STL35 having spherical dimples with a 35% are density ratio has shown the optimum tribological performance under the rotational speeds and normal load utilized in the present experimental study conducted under dry and solid lubricant coated conditions. Nonetheless, further research is needed to determine the optimum structure and density for dry and coated environments.

CONCLUSION

According to the literature review, dimple-texture patterns have proven to be an effective method of improving friction and wear properties of the tribo-contact pairs. The majority of studies focused on the influence of dimple-texturing on basic shapes like circles, squares, rectangles, and ellipses, and there is no study on honeycomb dimple-texture patterns. The key findings are presented below.

i. The experimental outcomes of an un-coated tungsten disk are compared to a MoS_2 coated tungsten disk; the frictional coefficient is significantly reduced in the MoS_2 coated tungsten disk due to the micro-dimple lubrication effect and the development of a thin layer of the solid lubricant on the tribo-contact pairs.

ii. At low rotational speeds, the wear rate is observed to be significantly high due to bulges of micro-dimples; however, at high rotational speeds, the bulges disappear, and the development of an oxide layer at the tribo-contact pairs influences the wear rate reduction. This phenomenon indicates that micro-cavities have a more significant impact on high-speed applications.

iii. Even though the influence tribological performance of non-textured and dimple-textured surfaces with different dimple area densities shows the non-linear behavior, the frictional coefficient values exhibit a linear relationship with the variation in rotational speed.

iv. MoS_2 coated surfaces perform significantly better than uncoated surfaces, with a 46~51% improvement in reducing frictional coefficient and a 51~55% improvement in reducing wear rate due to the micro-dimple lubrication effect and the formation of a thin layer of solid lubricant on the tribo-contact pairs.

v. MoS_2 coated spherical dimple-texture patterns perform much better than honeycomb dimple-texture patterns, resulting in a 40~45% wear reduction in dry condition and a 43~49% wear reduction in solid lubricant condition.

REFERENCES

[1] T. Ibatan, M. S. Uddin, and M. A. K. Chowdhury, "Recent development on surface texturing in enhancing tribological performance of bearing sliders," *Surf. Coat. Technol.*, vol. 272, no. June, pp. 102–120, 2015, doi: 10.1016/j.surfcoat.2015.04.017.

[2] Y. Xu *et al.*, "Influence of dimple shape on tribofilm formation and tribological properties of textured surfaces under full and starved lubrication," *Tribol. Int.*, vol. 136, no. August, pp. 267–275, 2019, doi: 10.1016/j.triboint.2019.03.047.

[3] S. Niketh, and G. L. Samuel, "Surface texturing of tribological interfaces–an experimental analysis," *Procedia Manuf.*, vol. 34, no. January, pp. 33–41, 2019, doi: 10.1016/j.promfg.2019.06.111

[4] G. Boidi *et al.*, "Effect of laser surface texturing on friction behaviour in elastohydrodynamically lubricated point contacts under different sliding-rolling conditions," *Tribol. Int.*, vol. 149, no. 105613, pp. 1–9, 2020, doi: 10.1016/j.triboint.2019.02.021.

[5] T. Liptakova, P. Fajnor, and M. Halamova, "Mechanical surface treatments effects on corrosion of AISI 316 Ti stainless steel in chloride environments," *J. Eng. Res.*, vol. 2, no. 20, pp. 196–210, 2014, doi: 10.7603/s40632-014-0020-1.

[6] J. Zhang *et al.*, "Frictional properties of surface textures fabricated on hardened steel by elliptical vibration diamond cutting," *Precis Eng.*, vol. 59, no. June, pp. 66–72, 2019, doi: 10.1016/J.PRECISIONENG.2019.06.001.

[7] Y. Arsyad *et al.*, "Laser surface modification of duplex stainless steel 2205 to modify the surface roughness," *Int. J. Automot. Mech. Eng.*, vol. 18, no. 2, pp. 8695–8703, 2021, doi: 10.15282/ijame.18.2.2021.07.0663.

[8] M. A. Hanafiah, A. A. Aziz, and A. R. Yusoff, "Influence of cutting parameters to surface area roughness in dimple machining using milling process," *Int. J. Automot. Mech. Eng.*, vol. 18, no. 3, pp. 9094–9100, 2021, doi: 10.15282/ijame.18.3.2021.21.0698.

[9] R. Meng *et al.*, "Modifying tribological performances of AISI 316 stainless steel surfaces by laser surface texturing and various solid lubricants," *Opt Laser Technol*, vol. 109, no. January, pp. 401–411, 2019, doi: 10.1016/j.optlastec.2018.08.020.

[10] H. K. Vuddagiri, S. Vadapalli, and J. Sagari, "Fabrication and modelling of tribological performance of Al-Si/12Al2O3/2MoS2 composite using taguchi technique," *Int. J. Automot. Mech. Eng.*, vol. 18, no. 3, pp. 8959–8977, 2021, doi: 10.15282/ijame.18.3.2021.09.0686.

[11] I. A. Ortega-Ramos *et al.*, "Effect of the surface texturing treatment with Nd: YAG laser on the wear resistance of CoCr alloy," *MRS Advances*, vol. 4, no. 55, pp. 3031–3039, 2019, doi: 10.1557/adv.2019.397.

[12] G. Fiaschi *et al.*, "Tribological response of laser-textured steel pins with low-dimensional micrometric patterns," *Tribol. Int.*, vol. 149, no. September, pp. 1–7, 2020, doi: 10.1016/j.triboint.2019.01.007.

[13] J. Zhang *et al.*, "Laser surface texturing of stainless steel− effect of pulse duration on texture's morphology and frictional response," *Adv. Eng. Mater.*, vol. 21, no. 3, pp. 1–7, 2018, doi: 10.1002/adem.201801016.

[14] K. Kartik Sriram, N. Radhika, M. Sam, and S. Shrihari, "Studies on adhesive wear characteristics of centrifugally cast functionally graded ceramic reinforced composite," *Int. J. Automot. Mech. Eng.*, vol. 17, no. 4, pp. 8274–8282, 2020, doi: 10.15282/ijame.17.4.2020.05.0625.

[15] J. J. Zhang *et al.*, "Surface textures fabricated by laser surface texturing and diamond cutting–influence of texture depth on friction and wear," *Adv. Eng. Mater.*, vol. 20, no. 4, pp. 1–8, 2018, doi: 10.1002/adem.201700995.

[16] M. Kumar, V. Ranjan, and R. Tyagi, "Effect of shape, density, and an array of dimples on the friction and wear performance of laser textured bearing steel under dry sliding," *J. Mater. Eng. Perform.,* vol. 29, no. May, pp. 2827–2838, 2020, doi: 10.1007/s11665-020-04816-8.

[17] S. P. Joshua, and P. D. Babu, "Effect of laser textured surface with different patterns on tribological characteristics of bearing material AISI 52100," *J. Cent. South Univ.*, vol. 27, no. 8, pp. 2210–2219, 2020, doi: 10.1007/s11771-020-4442-7.

[18] G. Vignesh, M. Prakash, M. D. Selvam, and P. Ragupathi, "Frictional performance of dimpled textured surfaces on a frictional pair: an experimental study," *i-Manager's J. Mech. Eng.*, vol. 8, no. 4, pp. 8–14, 2018, doi: 10.26634/jme.8.4.14337.

[19] D. Kummel, M. Hamann-Schroer, H. Hetzner, and J. Schneider, "Tribological behavior of nanosecond-laser surface textured Ti6Al4V," *Wear*, vol. 422, no. March, pp. 261–268, 2019, doi: 10.1016/j.wear.2019.01.079.

[20] N. Radhika, and M. Sam, "Statistical analysis of tribological performance of functionally graded copper composite using DOE," *Int. J. Automot. Mech. Eng.*, vol. 18, no. 3, pp. 8978–8985, 2021, doi: 10.15282/ijame.18.3.2021.10.0687.

[21] Y. Zhong, L. Zheng, Y. Gao, Z. Liu, "Numerical simulation and experimental investigation of tribological performance on bionic hexagonal textured surface" *Tribol. Int.*, vol. 129, no. January, pp. 151–161, 2019, doi: 10.1016/j.triboint.2018.08.010.

[22] M. D. Nikam, D. Shimpi, K. Bhole, and S. A. Mastud, "Design and development of surface texture for tribological application," *Key Eng. Mater.*, vol. 803, no. May, pp. 55–59, 2019, doi: 10.4028/www.scientific.net/KEM.803.55.

[23] G. Vignesh, D. Barik, P. Ragupathi, and S. Aravind, "Experimental analysis on turning of AISI 4340 steel using non-textured, dimple textured and MoS2 coated dimple textured carbide cutting inserts at the rack surface," *Mater. Today: Proc.*, vol. 33, no. 7, pp. 2616–2620, 2020, doi: 10.1016/j.matpr.2020.01.125.

[24] P. Lu *et al.*, "A novel surface texture shape for directional friction control," *Tribol. Lett.*, vol. 66, no. 51, pp. 1–13, 2018, doi: 10.1007/s11249-018-0995-0.

[25] R. Kataria, and J. Kumar, "A comparison of the different multiple response optimization techniques for turning operation of AISI O1 tool steel," *J. Eng. Res.*, vol. 2, no. 30, pp. 1–24, 2014, doi: 10.7603/s40632-014-0030-z.

[26] S. Yuan *et al.*, "Effect of laser surface texturing (LST) on tribological behavior of double glow plasma surface zirconizing coating on Ti6Al4V alloy," *Surf. Coat. Technol.*, vol. 368, no. June, pp. 97–109, 2019, doi: 10.1016/j.surfcoat.2019.04.038.

[27] L. Shi *et al.*, "Experimental investigation of the effect of typical surface texture patterns on mechanical seal performance," *J. Braz. Soc. Mech. Sci.*, vol. 42, no. 227, pp. 1–12, 2020, doi: 10.1007/s40430-020-02318-1.

[28] T. Stark *et al.*, "Positive effect of laser structured surfaces on tribological performance," *J. Laser Micro Nanoeng.*, vol. 14, no. 1, pp. 13–18, 2019, doi: 10.2961/jlmn.2019.01.0003.

[29] L. Chen, Z. Liu, Y. Li, and Z. Shi, "Effects of micro-milled malposed dimple structures on tribological behavior of Al-Si alloy under droplet lubricant condition," *Int. J. Adv. Manuf. Technol.*, vol. 98, no. September, pp. 143–150, 2018, doi: 10.1007/s00170-017-0603-8.

[30] B. Mao, A. Siddaiah, Y. Liao, and P. L. Menezes, "Laser surface texturing and related techniques for enhancing tribological performance of engineering materials: A review," *J. Manuf. Process.*, vol. 53, no. May, pp. 153–173, 2020, doi: 10.1016/j.jmapro.2020.02.009.

[31] G. Vignesh *et al.*, "Numerical investigation of dimple-texturing on the turning performance of hardened AISI H-13 steel," *Int. J. Simul. Multidiscip. Des. Optim.*, pp. 1–13, 2021, doi: 10.1051/smdo/2021043.

[32] G. Vignesh *et al.*, "An experimental study on machining of aisi h-13 steel using dimple-textured and non-textured tungsten carbide cutting tools," *In IOP Conference Series: Materials Science and Engineering*, vol. 1017, no. 1, pp. 012–021, 2021, doi: 10.1088/1757-899X/1017/1/012021.

[33] J. A. Wahab, M. J. Ghazali, W. M. Yusoff, and Z. Sajuri, "Enhancing material performance through laser surface texturing: a review" *Transactions of the IMF*, vol. 94, no. 4, pp. 193–198, 2016, doi: 10.1080/00202967.2016.1191141.

[34] K. N. Prasad, I. Syed, and S. K. Subbu, "Laser dimple texturing–applications, process, challenges, and recent developments: a review," *Aust. J. Mech. Eng.*, vol. 1, no. December, pp. 1–14, 2019, doi: 10.1080/14484846.2019.1705533.

[35] H. S. Hammood, S. S. Irhayyim, A. Y. Awad, and H. A. Abdulhadi, "Influence of multiwall carbon nanotube on mechanical and wear properties of copper–iron composite," *Int. J. Automot. Mech. Eng.*, vol. 17, no. 1, pp. 7570–7576, 2020, doi: 10.15282/ijame.17.1.2020.06.0561.